Peptidic degron in EID1 is recognized by an SCF E3 ligase complex containing the orphan F-box protein FBXO21

Cuiyan Zhang[a], Xiaotong Li[b], Guillaume Adelmant[c,d,e], Jessica Dobbins[f,g], Christoph Geisen[a,h], Matthew G. Oser[a], Kai W. Wucherpfenning[f,g], Jarrod A. Marto[c,d,e], and William G. Kaelin Jr.[a,h,1]

[a]Department of Medical Oncology, Dana-Farber Cancer Institute and Brigham and Women's Hospital, Harvard Medical School, Boston, MA 02215; [b]State Key Laboratory for Cellular Stress Biology, School of Life Sciences, Xiamen University, Xiamen, Fujian 361102, China; [c]Department of Cancer Biology, Dana-Farber Cancer Institute, Boston, MA 02215; [d]Blais Proteomics Center, Dana-Farber Cancer Institute, Boston, MA 02215; [e]Department of Biological Chemistry and Molecular Pharmacology, Harvard Medical School, Boston, MA 02215; [f]Department of Cancer Immunology and Virology, Dana-Farber Cancer Institute, Boston, MA 02215; [g]Department of Microbiology and Immunobiology, Harvard Medical School, Boston, MA 02215; and [h]Howard Hughes Medical Institute, Chevy Chase, MD 20815

Contributed by William G. Kaelin Jr., November 9, 2015 (sent for review October 24, 2015; reviewed by Bruce E. Clurman and Joan W. Conaway)

EP300-interacting inhibitor of differentiation 1 (EID1) belongs to a protein family implicated in the control of transcription, differentiation, DNA repair, and chromosomal maintenance. EID1 has a very short half-life, especially in G0 cells. We discovered that EID1 contains a peptidic, modular degron that is necessary and sufficient for its polyubiquitylation and proteasomal degradation. We found that this degron is recognized by an Skp1, Cullin, and F-box (SCF)-containing ubiquitin ligase complex that uses the F-box Only Protein 21 (FBXO21) as its substrate recognition subunit. SCF^{FBXO21} polyubiquitylates EID1 both in vitro and in vivo and is required for the efficient degradation of EID1 in both cycling and quiescent cells. The EID1 degron partially overlaps with its retinoblastoma tumor suppressor protein-binding domain and is congruent with a previously defined melanoma-associated antigen-binding motif shared by EID family members, suggesting that binding to retinoblastoma tumor suppressor and melanoma-associated antigen family proteins could affect the polyubiquitylation and turnover of EID family members in cells.

degradation | ubiquitylation | cell cycle | G0 | pRB

Regulation of protein abundance through alterations in protein stability plays a critical role in cellular homeostasis. For many proteins, stability is governed by the concerted actions of dedicated ubiquitin ligases, which promote proteasomal degradation, and deubiquitinating enzymes, which oppose them. There are thought to be over 500 potential ubiquitin ligases and ∼100 deubiquitinating enzymes (1, 2).

Many ubiquitin ligases belong to the Skp1, Cullin, and F-box (SCF) family, characterized by the presence of S-phase kinase-associated protein 1 (Skp1), Cullin-1 (Cul1), and an F-box protein, with the latter serving as the substrate recognition subunit (3, 4). F-box proteins contain the collinear motif for which they are named and, frequently, a dedicated protein-binding motif such as a WD40 domain. F-box proteins lacking such protein-binding domains are referred to as F-box only proteins. Archetypal SCF complexes include the SCF complex containing the F-box protein Skp2, which polyubiquitylates proteins such as the cell-cycle regulators p27 and cyclin E, and the SCF complex containing Fbw7, which polyubiquitylates proteins such as c-Jun and c-Myc (1).

EP300-interacting inhibitor of differentiation 1 (EID1) is a short-lived protein with a half-life measured in minutes, especially as cells exit the cell cycle (5, 6). It was originally identified by virtue of its ability to bind to the retinoblastoma tumor suppressor protein (pRB) and contains an LXCXE pRB-binding motif first identified in the viral oncoproteins adenovirus E1A, SV40 large T, and human papillomavirus E7 (5-9). Structural studies suggest that EID1 makes two contacts with pRB, one involving the pRB N terminus and one involving the LXCXE-binding domain within the pRB C terminus (10). EID1 also binds to small heterodimer partner (SHP) [also called NR0B2 (nuclear receptor subfamily 0, group B, member 2)], which is a transcriptional corepressor for various steroid hormone family transcription factors (11–14). In cell-based models, overexpression of EID1 likewise represses transcription factors and blocks differentiation (5, 6, 11, 14–17). These cellular activities correlate with its ability to inhibit p300 histone acetyltransferase in vitro and in vivo (5, 6, 11).

Proteins with very short half-lives often perform important functions that justify the energetic cost of their continuous synthesis and degradation. Previous studies of EID1 function relied heavily on exogenous overexpression, which could introduce artifacts caused by nonphysiological protein abundance. In an attempt to control EID1 abundance in a more physiological manner, and to begin to understand its normal functions, we sought to identify the ubiquitin ligase for EID1.

Results

Previous structure-function studies showed that the EID1 C terminus is required both for its polyubiquitylation and for its ability to bind to the mouse double minute 2 homolog (MDM2)

Significance

Many short-lived proteins perform important cellular functions that must be tightly regulated. EID1 is an unstable protein implicated in the control of transcription, differentiation, and genomic integrity. EID1 is particularly unstable in G0 cells. Here we show that an SCF complex containing the orphan F-box only protein FBXO21 is the ubiquitin ligase that recognizes EID1 in both cycling and G0 cells and that it recognizes a modular, peptidic domain within EID1. This degron overlaps with the EID1 region that binds to the retinoblastoma tumor suppressor protein (pRB) and to melanoma-associated antigen (MAGE) proteins, suggesting that multiple proteins compete for binding to EID1 and secondarily influence its ubiquitinylation. This study sheds light on the regulation of EID1, the function of FBXO21, and control of protein turnover by ubiquitin ligases.

Author contributions: C.Z. and W.G.K. designed research; C.Z., X.L., G.A., J.D., C.G., M.G.O., K.W.W., and J.A.M. performed research; X.L. generated initial degron mapping data; G.A. and J.A.M. performed mass spectrometry analysis; J.D. and K.W.W. isolated and stimulated T cells; C.G. assisted with mammalian two-hybrid assays; M.G.O. generated and validated the small guide RNAs targeting MDM2; W.G.K. conceived and supervised research; C.Z. analyzed data; and C.Z. and W.G.K. wrote the paper.

Reviewers: B.E.C., Fred Hutchinson Cancer Research Center; and J.W.C., Stowers Institute for Medical Research.

The authors declare no conflict of interest.

[1]To whom correspondence should be addressed. Email: william_kaelin@dfci.harvard.edu.

This article contains supporting information online at www.pnas.org/lookup/suppl/doi:10.1073/pnas.1522006112/-/DCSupplemental.

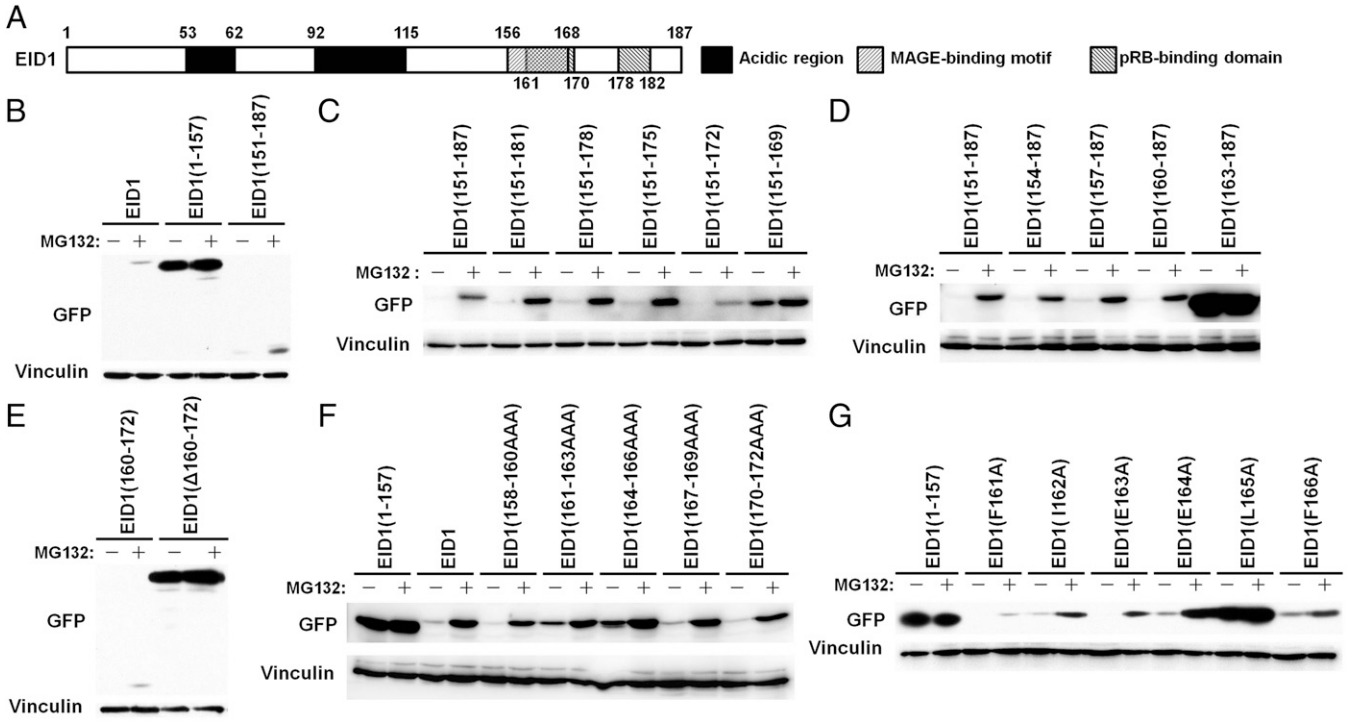

Fig. 1. Mapping of EID1 degron. (*A*) EID1 schematic. (*B–G*) Anti-GFP immunoblot analysis of HeLa cells transiently transfected to produce the indicated GFP-EID1 fusion proteins and then treated or untreated with 10 μM MG132 overnight as indicated.

ubiquitin ligase, suggesting the two properties are linked (5). Moreover, exogenously expressed MDM2 polyubiquitylates EID1 in cells (5, 18). On the other hand, we found that EID1 was rapidly polyubiquitylated and degraded in $p53^{-/-};Mdm2^{-/-}$ mouse embryo fibroblasts, strongly suggesting the existence of another EID1 ubiquitin ligase. In addition, two studies showed that EID1 is dramatically induced by MLN4924, which inhibits the NEDD8 activating enzyme and hence cullin-dependent ubiquitin ligases (19, 20). Together, these observations suggested that EID1 is polyubiquitylated by a cullin-dependent ubiquitin ligase instead of, or perhaps in addition to, MDM2.

We tried to define the minimal EID1 degron as a prelude to identifying the EID1 ubiquitin ligase. Toward this end, we transiently expressed various fragments of EID1, fused to the C terminus of green fluorescent protein (GFP), in HeLa cells and monitored their accumulation in the presence and absence of the proteasomal inhibitor MG132 by anti-GFP immunoblot analysis. EID1 contains 187 amino acid residues (Fig. 1*A*). Consistent with prior work, an EID1 mutant [EID1(1–157)] lacking its extreme C terminus accumulated to very high levels compared with wild-type EID1 and was largely insensitive to MG132 (Fig. 1*B*). In contrast, the behavior of GFP-fused EID1 residues 151–187 was indistinguishable from that of GFP-fused to full-length EID1 in these assays, being produced at very low levels in untreated cells and induced by MG132 (Fig. 1*B*). Therefore, the EID1 C terminus is both necessary and sufficient for the proteasomal degradation of EID1.

We then performed fine-mapping studies using a nested set of C-terminal and N-terminal EID1(151–187) truncation mutants fused to the GFP C terminus. Progressive elimination of C-terminal residues from EID1(151–187) revealed that EID1 residues 173–187 are dispensible for proteasomal degradation of EID1 (Fig. 1*C*). In contrast, eliminating residues 170–187 stabilized EID1 (Fig. 1*C*). Conversely, progressive elimination of N-terminal residues from EID1(151–187) showed that residues 151–159 are dispensible for proteasomal degradation of EID, whereas eliminating residues 151–162 stabilized EID1 (Fig. 1*D*). This latter result needs to be interpreted cautiously as the presence of the GFP moiety could have steric effects on the N terminus of the EID1 degron. Specifically, some N-terminal EID1 amino acids in the fusions could be acting as spacers. This concern, however, is largely mitigated by experiments described below.

Consistent with these results, GFP fused to EID1 160–172 was apparently unstable and induced by MG132, whereas in-frame deletion of EID1 residues 160–172 stabilized otherwise full-length

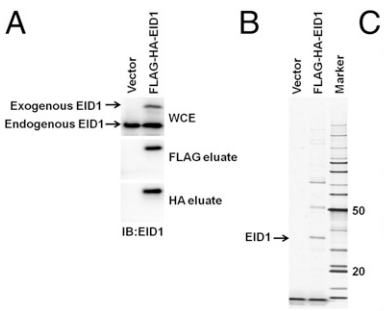

C

Entrez Gene Symbol	Protein Description	Unique Sequences	Spectral Count
EID1	EP300-interacting inhibitor of differentiation 1 [Homo sapiens]	5	78
JAK1	tyrosine-protein kinase JAK1 [Homo sapiens]	9	15
IQGAP1	ras GTPase-activating-like protein IQGAP1 [Homo sapiens]	5	6
KIAA1543	calmodulin-regulated spectrin-associated protein 3 isoform 1 [Homo sapiens]	3	3
DNAJA1	dnaJ homolog subfamily A member 1 [Homo sapiens]	2	2
TESK2	dual specificity testis-specific protein kinase 2 [Homo sapiens]	1	1
PFKP	6-phosphofructokinase type C isoform 1 [Homo sapiens]	1	1
SCAF11	protein SCAF11 [Homo sapiens]	1	1
C14orf156	SRA stem-loop-interacting RNA-binding protein, mitochondrial precursor [Homo sapiens]	1	1
DMBT1	deleted in malignant brain tumors 1 protein isoform a precursor [Homo sapiens]	1	1
FBXO21	F-box only protein 21 isoform 2 [Homo sapiens]	1	1
RPL21	60S ribosomal protein L21 [Homo sapiens]	1	1
DISP1	protein dispatched homolog 1 [Homo sapiens]	1	1
RASA3	ras GTPase-activating protein 3 [Homo sapiens]	1	1
RCN2	reticulocalbin-2 precursor [Homo sapiens]	1	1
RPL37A	60S ribosomal protein L37a [Homo sapiens]	1	1
PCNT	pericentrin [Homo sapiens]	1	1

Fig. 2. EID1 copurifies with FBXO21. (*A*) Anti-EID1 immunoblot analysis of whole-cell extracts (WCEs) of HeLa cells stably infected with a pBABE-based retrovirus encoding Flag-HA-EID1 or with the empty vector (*Top*), Flag peptide eluate after anti-Flag immunoprecipitation (*Middle*), and HA peptide eluate after anti-HA immunoprecipitation of the Flag eluate (*Bottom*). (*B*) Silver stain of final HA peptide eluates from cells treated as in *A*. (*C*) Peptides detected by MS/MS analysis of HA peptide eluates as in *B*.

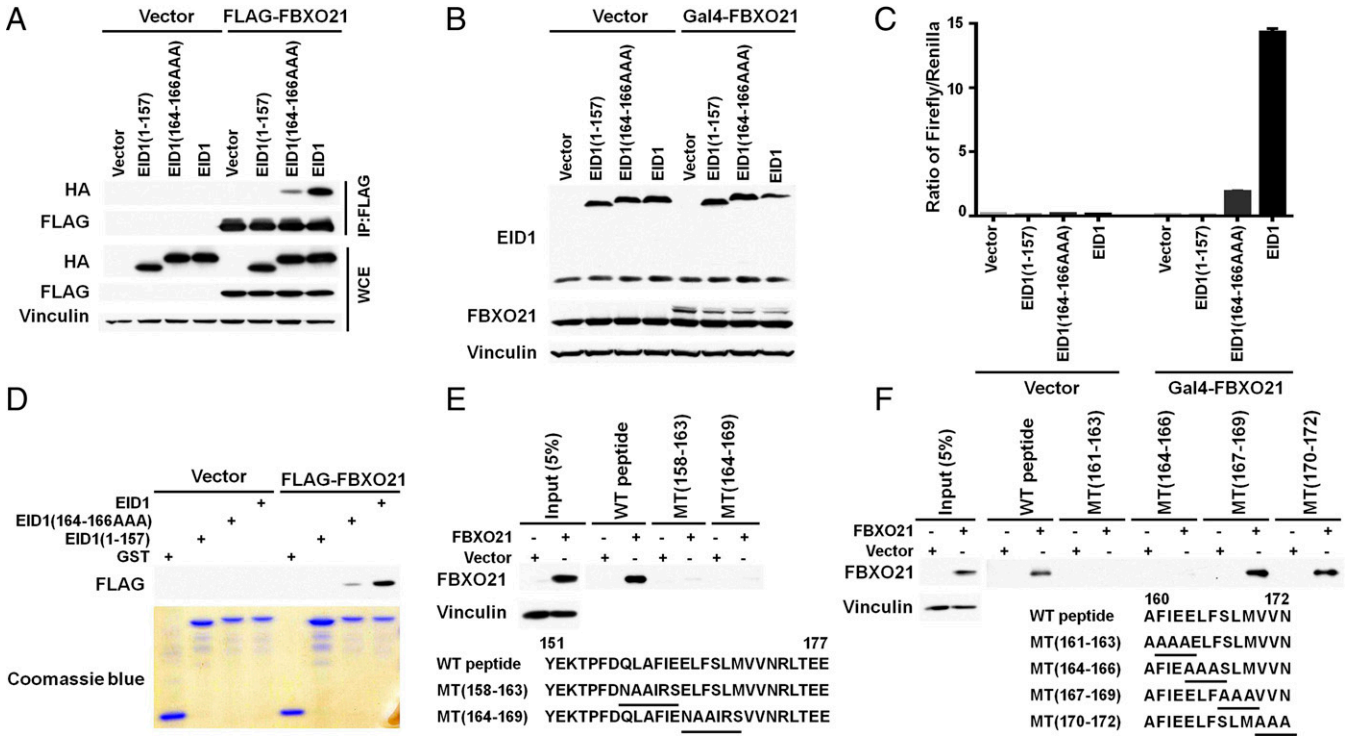

Fig. 3. FBXO21 binds to the EID1 degron. (*A*) Immunoblot analysis of WCEs and anti-Flag immunoprecipitates (IP:Flag) prepared from 293FT cells transfected with a plasmid encoding Flag-FBXO21 or the empty vector together with a plasmid encoding the indicated HA-EID1 variants or empty vector. Cells were treated with MG132 for 3 h before lysis. (*B*) Immunoblot analysis of 293FT cells transfected with a plasmid encoding Gal4-FBXO21 or the empty vector together with a plasmid encoding the indicated EID1–VP16 fusion proteins (or empty vector), a plasmid encoding renilla luciferase, and a reporter plasmid containing Gal4 DNA-binding sites upstream of firefly luciferase. (*C*) Normalized firefly luciferase values for cells treated as in *B* 24 h after transfection. (*D*) Anti-Flag immunoblot (*Top*) of Flag-FBXO21 in vitro translate bound to the indicated GST-EID1 fusion proteins. Comparable recovery of the GST fusion proteins was confirmed by Coomassie blue staining (*Bottom*). (*E* and *F*) Anti-FBXO21 immunoblot analysis of Flag-FBOX21 produced in 293FT cells and bound to the indicated EID1(151–177) (*E*) and EID(160–172) (*F*) biotinylated peptides. The 293FT cells transfected with empty vector were included as controls.

EID1 (Fig. 1*E* and Fig. S1). Finally, we performed an alanine scan in the context of full-length EID1 focused on residues 160–172, changing three sequential residues to alanine at a time. Converting EID1 residues 158–160, 167–169, or 170–172 to three alanines (AAA) had no discernable effect on EID1 degradation (Fig. 1*F*). In contrast, converting EID1 residues 161–163, and especially 164–166, to AAA partially stabilized EID1 (Fig. 1*F*). A more focused alanine scan, changing one alanine at a time, showed that L165 was required for the rapid turnover of EID1 (Fig. 1*G*).

To identify the relevant ubiquitin ligase, we stably infected HeLa cells with a retrovirus encoding exogenous EID1 with both a Flag epitope and hemagglutinin (HA) epitope tag at its N terminus (pBABE-Flag-HA-EID1) or the empty vector (vector) (Fig. 2*A*), treated the cells with MG132 overnight, and performed a preparative immunoprecipitation with anti-Flag Sepharose. Bound proteins were eluted with a Flag epitope peptide and then immunoprecipitated with anti-HA Sepharose, eluted with an HA epitope peptide, and analyzed by silver staining (Fig. 2*B*) and by mass spectrometry (MS) (Fig. 2*C*). The presence of EID1 in the sequential Flag and HA eluates was confirmed by immunoblot analysis (Fig. 2*A*). MS analysis of the final HA eluate from cells expressing Flag-HA-EID1 revealed the presence of multiple proteins, including the F-box Only Protein 21 (FBXO21) (Fig. 2*C* and Fig. S2). We pursued FBXO21 because F-box proteins often serve as substrate recognition modules in SCF ubiquitin ligases.

In cotransfection experiments, we confirmed that exogenous FBXO21 can bind to EID1 in cells. In one set of experiments, 293FT cells were cotransfected to produce HA-EID1 and Flag-FBXO21 and treated with MG132. EID1 was detected, as determined by anti-HA immunoblot analysis, in anti-Flag immunoprecipitates (Fig. 3*A*). The recovery of HA-EID1 required the presence of Flag-FBXO21 and was specific because binding of HA-EID1 (164–166AAA) and HA-EID1(1–157) to Flag-FBXO21 was diminished and absent, respectively, in these assays (Fig. 3*A*). Similarly, wild-type EID1, but neither EID1(164–166AAA) nor EID1(1–157), bound to FBOX21 in mammalian two-hybrid assays in which EID1 was expressed as the prey protein fused to VP16 and FBXO21 was used as the bait fused to the Gal4 DNA-binding domain (Fig. 3 *B* and *C*).

To ask if FBXO21 could bind to recombinant EID1, we performed GST–pull-down assays with recombinant GST-EID1 fusion proteins. Flag-FBXO21 produced by in vitro translation specifically bound to GST-EID1 but bound poorly to GST-EID1(164–166AAA) and undetectably to GST-EID1(1–157) (Fig. 3*D*). Comparable recovery of the different GST fusion proteins was confirmed by Coomassie blue staining (Fig. 3*D*).

Finally, we did binding assays with biotinylated EID1 peptides. Flag-FBXO21 produced in 293T cells by transient transfection bound to synthetic EID1 peptides corresponding to EID1 residues 151–177 or the minimal degron 160–172 (Fig. 3 *E* and *F*, respectively). Consistent with our degron alanine scanning experiments, replacement of residues 158–163 or residues 164–169 with a flexible linker (NAAIRS) (21) in the EID1 151–177 peptide abrogated FBXO21 binding, as did replacement of residues 161–163 or 164–166 in the EID1 160–172 peptide with three consecutive alanine residues (Fig. 3 *E* and *F*).

Next we performed in vitro and in vivo ubiquitylation assays. For the former, 293FT cells were transfected to produce Myc epitope-tagged versions of wild-type FBXO21, an F-box deleted version of FBXO21(FBXO21ΔF), or were transfected with an

empty vector. We then performed in vitro ubiquitylation assays with the anti-Myc immunoprecipitates and ^{35}S-labeled EID1 produced by in vitro translation with rabbit reticulocyte lysates. Myc-FBXO21, but not Myc-FBXO21ΔF, immunoprecipitates ubiquitylated EID1 when supplemented with a recombinant E1 ubiqutin-activating enzyme and an E2 ubiquitin-conjugating enzyme (Fig. 4*A*). This was specific because ubiquitylation of EID1 (164–166AAA) was greatly diminished compared with wild-type EID1, and ubiquitylation of EID1(1–157) was undetectable (Fig. 4*B*). Similarly, wild-type FBXO21 promoted the ubiquitylation of wild-type T7-EID1 in vivo, as determined by the presence of HA-tagged ubiquitin in anti-T7 immunoprecipitates performed under denaturing conditions from cells in which the proteasome was inhibited by MG132 (Fig. 4 *C* and *D*). As was true in the in vitro assays, ubiquitylation of EID1(164–166AAA) and EID1 (1–157) by FBOXO21 in vivo was greatly diminished and absent, respectively, compared with wild-type EID1 (Fig. 4 *C* and *D*).

Next we stably infected 293FT cells to produce Flag-HA-FBXO21 and identified FBXO21-associated proteins in the presence of MG132 by sequential preparative immunoprecipitations with anti-Flag and anti–HA-Sepharose followed by MS. MS revealed the presence of peptides from Skp1 and Cul1 in addition to peptides from EID1 and its paralog EP300-interacting inhibitor of differentiation 2 (EID2) (Fig. S3*A*). Notably, the EID1 degron described above is well conserved in EID2 (Fig. S3*B*). Coimmunoprecipitation of Skp1 and Cul1 with FBXO21 was confirmed by immunoblot analysis (Fig. 5*A*). These findings suggested that FBXO21 is the substrate recognition subunit of a canonical SCF ubiquitin ligase complex and strengthened the idea that EID1 is one of its substrates.

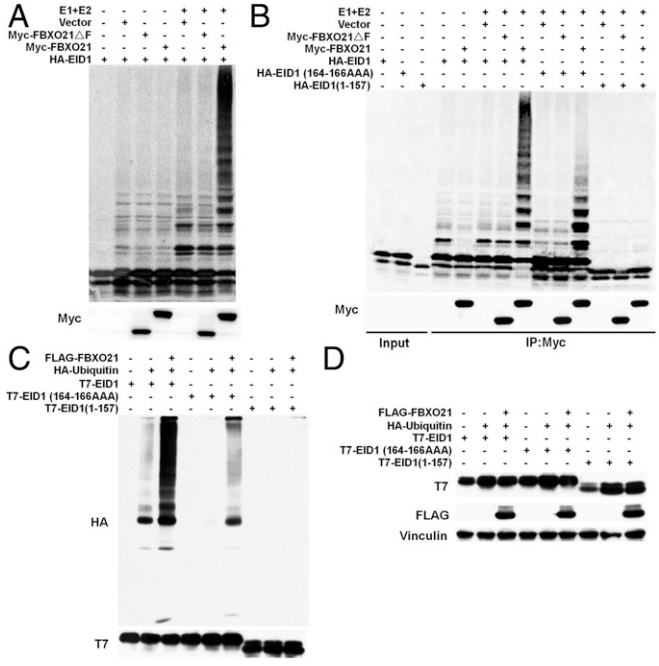

Fig. 4. Polyubiquitylation of EID1 by an FBXO21. (*A* and *B*) Autoradiogram (*Top*) of the indicated ^{35}S HA-EID1 in vitro translates after incubation with anti-Myc immunoprecipitates from 293FT cells transfected to produce Myc-FBXO21, Myc-FBXO21ΔF-box, or with the empty vector, in the presence or absence of recombinant E1 and E2, as indicated. Comparable recovery of Myc-tagged proteins was confirmed by immunoblot analysis (*Bottom*). In *B*, ubiquitylation assays performed with a mock immunoprecipitate lacking a primary antibody (beads only) were included as an additional negative control. Lanes labeled input equal one-third of the in vitro translate amount used in the ubiquitylation assays. (*C*) Anti-HA (*Top*) and anti-T7 (*Bottom*) immunoblots of anti-T7 immunoprecipitates from 293FT cells transfected to produce Flag-FBXO21, HA-ubiquitin, and T7-EID1 variants, as indicated. (*D*) Immunoblots of WCEs used in *D*.

We used several approaches to ask whether SCF^{FBXO21} regulates EID1 turnover in cells. Consistent with two recent studies (19, 20), MLN4924 robustly induced the accumulation of endogenous EID1, implicating an SCF ubiquitin ligase in the control of EID1 turnover (Fig. 5*B*). Down-regulation of *FBXO21* or *Cul1* with effective small interfering RNAs (siRNAs) induced the accumulation of endogenous EID1 (Fig. 5 *C* and *D* and Fig. S4). These effects were specific because effective siRNAs against other F-box only proteins or cullins did not induce EID1 (Fig. 5 *C* and *D* and Fig. S4 *A*–*D*). Similarly, siRNAs against *FBXO21* and *Cul1* induced the accumulation of exogenous EID1 but had little or no effect on EID1(164–166AAA) (Fig. 5*E*). MDM2 has also been reported to regulate EID1 turnover cells (5, 18), but we did not observe robust induction of EID1 with an effective *MDM2* siRNA, either alone or in combination with an *FBXO21* siRNA (Fig. 5*E* and Fig. S4 *E* and *F*). Consistent with our siRNA results, stable knockdown of *FBXO21* with multiple independent small hairpin RNAs (shRNAs) (Fig. 5*F*) or with CRISPR-associated protein 9 (Cas9) and multiple independent *FBXO21* small guide RNAs (sgRNAs) induced the accumulation of EID1 (Fig. 5*G*). In contrast, but in keeping with our siRNA results, Cas9-mediated knockdown of *MDM2* did not induce EID1 but did induce the canonical MDM2 target p53 (Fig. 5*G*).

As expected, the accumulation of EID1 in cells lacking *FBXO21* was linked to increased EID1 stability, as determined by its rate of disappearance in cells treated with cycloheximide (CHX) (Fig. 5*H*), and was posttranscriptional, as evidenced by increased firefly luciferase activity in cells transfected with a bicistronic reporter plasmid encoding an EID1–firefly luciferase fusion protein and renilla luciferase (22) (Fig. 5*I* and Fig. S5).

EID1 protein abundance falls as cells exit the cell cycle (5, 6). To ask whether cells that have not previously entered the cell cycle regulate EID1 at the G0/1 transition, we stimulated resting T cells to enter the cell cycle and monitored EID1 protein levels. EID1 protein was barely detectable in resting T cells but was induced 12–24 h after T-cell receptor activation, which stimulates cell-cycle entry, without a corresponding change in EID1 mRNA abundance (Fig. 6 *A* and *B*). EID1 protein levels were also induced in G0 cells by the proteasome inhibitor MG132 (Fig. 6*C*). Therefore, EID1 protein levels are regulated upon both entry into and exit from the cell cycle.

To ask if SCF^{FBXO21} regulates EID1 in both G0 and cycling cells, we analyzed T98G glioblastoma cells and WI-38 human fibroblasts that were serum-starved into G0 or maintained in serum. Under both conditions EID1 was induced by Cas9-mediated elimination of *FBXO21* with two different effective sgRNAs (Fig. 6 *D* and *E* and Fig. S6 *A* and *B*). In a complementary set of experiments, we transiently transfected T98G stably producing a bicistronic EID–luciferase stability reporter with an effective *FBXO21* siRNA or a control siRNA and then grew the cells for 72 h in the presence or absence of serum. EID1 stability, as measured by firefly/renilla luciferase ratio, decreased in serum-starved cells treated with the control siRNA but not *FBXO21* siRNA (Fig. 6 *F* and *G* and Fig. S6*C*). Notably, FBXO21 is present in both G0 cells and in cycling cells. In some, but not all, cells, we observed a modest increase in FBXO21 levels in G0 compared with cycling cells (Fig. 6 *C*–*E*). We have not, under the assay conditions tested to date, detected a decrease in FBXO21 ubiquitin ligase activity in cycling cells compared with G0 cells nor changes in the subcellular localizations of FBXO21 and EID1 under these two conditions. It will be important to determine how, mechanistically, EID1 levels increase in cycling cells.

Discussion

Our studies show that SCF^{FBXO21} is a ubiquitin ligase for EID1. The same conclusion has now been reported by another group

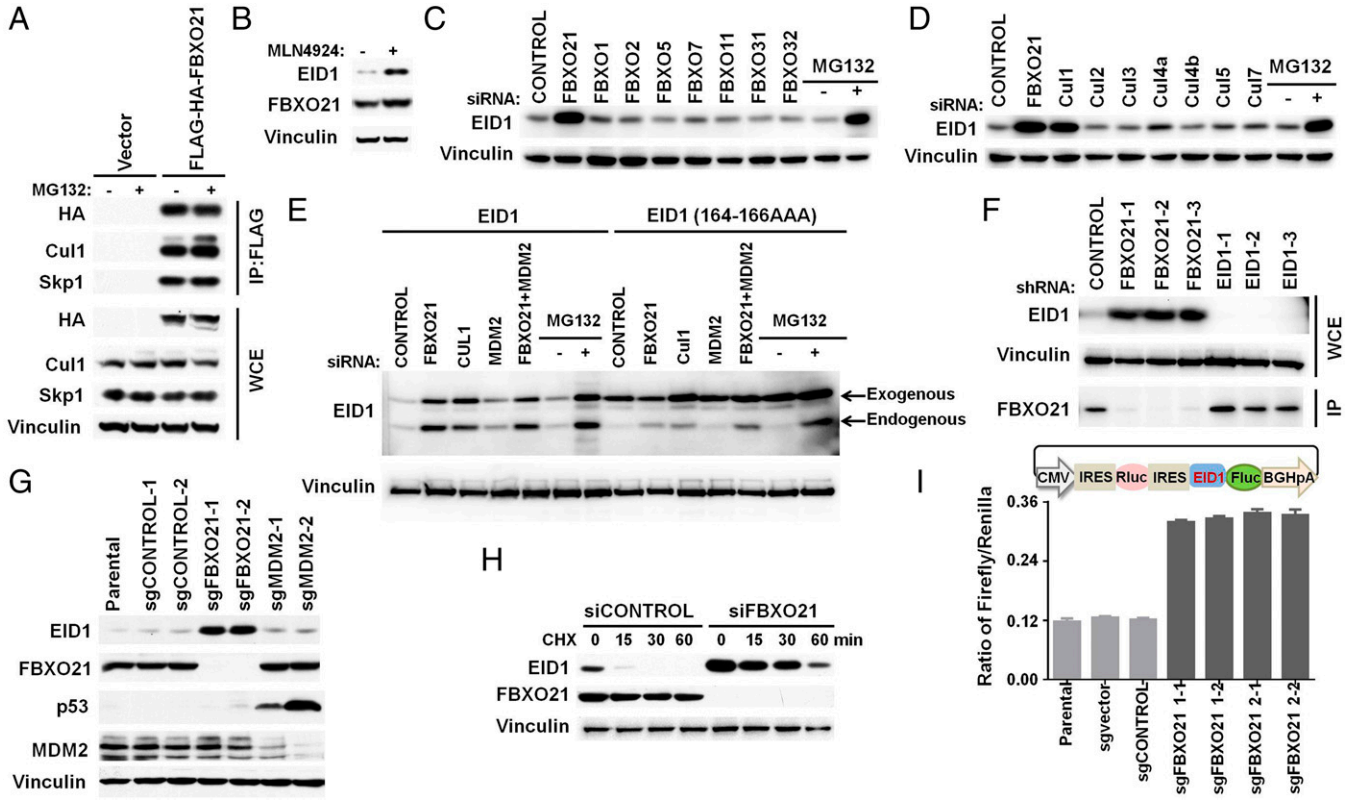

Fig. 5. SCF^{FBXO21} regulates EID1 turnover in cells. (*A*) Immunoblot analysis of WCEs and anti-Flag immunoprecipitates (IP:Flag) prepared from 293FT cells stably infected to express Flag-HA-FBXO21 or the empty vector. MG132 was added for 3 h where indicated. (*B*) Immunoblot analysis of U2OS cells treated with MLN4924 for 4 h. (*C–E*) Immunoblot analysis of 293FT cells transfected with the indicated siRNAs. In *E*, cells were retrovirally infected to stably produce the indicated HA-EID1 variants. (*F*) Immunoblot analysis of 293FT cells infected to produce the indicated shRNAs. IP, endogenous FBXO21 immunoprecipitate; WCE, whole-cell extract. (*G*) Immunoblot analysis of A549 cells infected to produce Cas9 and the indicated sgRNAs. (*H*) Immunoblot analysis of 293FT cells transfected with the indicated siRNAs and then treated with CHX for the indicated duration. (*I*) Normalized luciferase values after transfecting 293FT cells as in *G* with a plasmid encoding EID1 fused to firefly luciferase and renilla luciferase from a bicistronic mRNA.

working in parallel (23, 24). Despite earlier reports (5, 18), we have thus far not confirmed a physiological role for MDM2 in EID1 ubiquitylation, although MDM2 might polyubiquitylate EID1 under conditions not tested here.

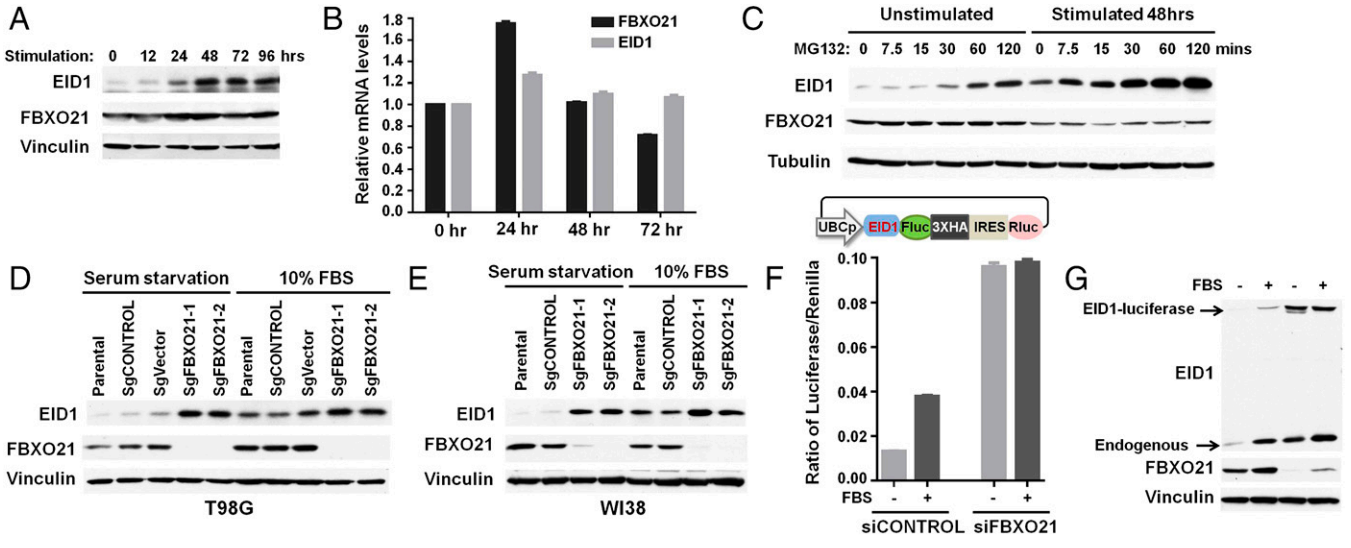

Fig. 6. SCF^{FBXO21} is required for degradation of EID1 in G0. (*A–C*) Immunoblot analysis (*A* and *C*) and mRNA levels (*B*) of resting T cells induced to enter the cell cycle with anti-CD3 (cluster of differentiation 3) and anti-CD28 (cluster of differentiation 28) antibodies. In *C*, cells were also treated with MG132 for the indicated duration before cell lysis. (*D* and *E*) Immunoblot analysis of T98G (*D*) and WI-38 (*E*) cells grown under serum-poor and serum-replete conditions. (*F* and *G*) Normalized luciferase values (*F*) and immunoblot analysis (*G*) of T98G cells stably expressing an EID1–luciferase stability reporter after transfection with the indicated siRNAs and growth in the presence or absence of serum for 72 h.

EID1 has several paralogs including EID2, EID2B, and EID3 (25–32). The EID1 degron identified here is well conserved among the EID family members, and EID2 coimmunoprecipitates with FBXO21 in cells treated with MG132. It is therefore likely that SCF^{FBXO21} regulates other EID family members.

The binding of SCF complexes to their substrates is often regulated by posttranslational degron modifications. The EID1 degron we identified here is not known to be modified and, as a synthetic, presumably unmodified, peptide binds to FBXO21. It remains possible that the EID1 degron is modified under certain circumstances, leading to altered recognition by FBXO21 or that regulatory signals impinge upon SCF^{FBXO21} rather than its substrates.

In overexpression studies, EID family members can repress transcription mediated by various DNA-binding transcription factors, perhaps by inhibiting p300 and CBP, and can block differentiation. On the other hand, we have thus far been unable to replicate these EID1-induced phenotypes by inactivating FBXO21, suggesting that they were artifacts caused by EID1 overexpression or that FBXO21 loss has additional effects that mitigate the consequences of increased EID abundance.

Finally, it has been suggested that the EID and melanoma-associated antigen (MAGE) proteins are mammalian counterparts of yeast Nse4 and Nse3, respectively, which form an SMC complex involved in chromatin maintenance and DNA repair (30, 32). Conceivably this function provides a teleological explanation for the induction of EID proteins during the cell cycle. Moreover, the EID1 degron recognized by FBXO21 is essentially congruent with the MAGE/Nse3-binding motif identified by others. Perhaps binding to MAGE/Nse3-like proteins shields EID1 from FBXO21 during the cell cycle. The ability of the MAGE-related protein Necdin to bind to and stabilize EID1 is consistent with this idea (16). Similarly, the EID1 degron overlaps with the EID1 pRB-binding region, suggesting that EID1 stability could also be influenced by pRB and providing a mechanistic explanation for the induction of EID1 in cells observed after exogenous pRB expression (5).

ACKNOWLEDGMENTS. We thank Gang Lu for the luciferase fusion reporter plasmids and members of the W.G.K. laboratory for useful discussions and careful reading of the manuscript. This work was supported by an NIH grant (to W.G.K.) and Dana-Farber Strategic Research Initiative and NINDS (J.A.M.). W.G.K. is a Howard Hughes Medical Institute investigator.

1. Nakayama KI, Nakayama K (2006) Ubiquitin ligases: Cell-cycle control and cancer. *Nat Rev Cancer* 6(5):369–381.
2. Reyes-Turcu FE, Ventii KH, Wilkinson KD (2009) Regulation and cellular roles of ubiquitin-specific deubiquitinating enzymes. *Annu Rev Biochem* 78:363–397.
3. Deshaies RJ (1999) SCF and Cullin/Ring H2-based ubiquitin ligases. *Annu Rev Cell Dev Biol* 15:435–467.
4. Lydeard JR, Schulman BA, Harper JW (2013) Building and remodelling Cullin-RING E3 ubiquitin ligases. *EMBO Rep* 14(12):1050–1061.
5. Miyake S, et al. (2000) Cells degrade a novel inhibitor of differentiation with E1A-like properties upon exiting the cell cycle. *Mol Cell Biol* 20(23):8889–8902.
6. MacLellan W, Xiao G, Abdellatif M, Schneider M (2000) A novel Rb- and p300-binding protein inhibits transactivation by MyoD. *Mol Cell Biol* 20(23):8903–8915.
7. Wen H, Ao S (2001) Identification and characterization of a novel human cDNA encoding a 21 kDa pRb-associated protein. *Gene* 263(1-2):85–92.
8. Nguyen DX, Baglia LA, Huang SM, Baker CM, McCance DJ (2004) Acetylation regulates the differentiation-specific functions of the retinoblastoma protein. *EMBO J* 23(7):1609–1618.
9. Krützfeldt M, et al. (2005) Selective ablation of retinoblastoma protein function by the RET finger protein. *Mol Cell* 18(2):213–224.
10. Hassler M, et al. (2007) Crystal structure of the retinoblastoma protein N domain provides insight into tumor suppression, ligand interaction, and holoprotein architecture. *Mol Cell* 28(3):371–385.
11. Båvner A, Johansson L, Toresson G, Gustafsson JA, Treuter E (2002) A transcriptional inhibitor targeted by the atypical orphan nuclear receptor SHP. *EMBO Rep* 3(5): 478–484.
12. Zhou T, et al. (2010) Novel polymorphisms of nuclear receptor SHP associated with functional and structural changes. *J Biol Chem* 285(32):24871–24881.
13. Zhi X, et al. (2014) Structural insights into gene repression by the orphan nuclear receptor SHP. *Proc Natl Acad Sci USA* 111(2):839–844.
14. Zhang Y, et al. (2014) E2F1 is a novel fibrogenic gene that regulates cholestatic liver fibrosis through the Egr-1/SHP/EID1 network. *Hepatology* 60(3):919–930.
15. Lizcano F, Vargas D (2010) EID1-induces brown-like adipocyte traits in white 3T3-L1 pre-adipocytes. *Biochem Biophys Res Commun* 398(2):160–165.
16. Bush JR, Wevrick R (2008) The Prader-Willi syndrome protein necdin interacts with the E1A-like inhibitor of differentiation EID-1 and promotes myoblast differentiation. *Differentiation* 76(9):994–1005.
17. Park YY, et al. (2007) EID-1 interacts with orphan nuclear receptor SF-1 and represses its transactivation. *Mol Cells* 24(3):372–377.
18. Ye B, et al. (2014) Pcid2 inactivates developmental genes in human and mouse embryonic stem cells to sustain their pluripotency by modulation of EID1 stability. *Stem Cells* 32(3):623–635.
19. Liao H, et al. (2011) Quantitative proteomic analysis of cellular protein modulation upon inhibition of the NEDD8-activating enzyme by MLN4924. *Mol Cell Proteomics* 10(11):M111.009183.
20. Emanuele MJ, et al. (2011) Global identification of modular cullin-RING ligase substrates. *Cell* 147(2):459–474.
21. Wilson IA, et al. (1985) Identical short peptide sequences in unrelated proteins can have different conformations: A testing ground for theories of immune recognition. *Proc Natl Acad Sci USA* 82(16):5255–5259.
22. Lu G, et al. (2014) The myeloma drug lenalidomide promotes the cereblon-dependent destruction of Ikaros proteins. *Science* 343(6168):305–309.
23. Yoshida Y, et al. (2015) A comprehensive method for detecting ubiquitinated substrates using TR-TUBE. *Proc Natl Acad Sci USA* 112(15):4630–4635.
24. Watanabe K, Yumimoto K, Nakayama KI (2015) FBXO21 mediates the ubiquitylation and proteasomal degradation of EID1. *Genes Cells* 20(8):667–674.
25. Miyake S, Yanagisawa Y, Yuasa Y (2003) A novel EID-1 family member, EID-2, associates with histone deacetylases and inhibits muscle differentiation. *J Biol Chem* 278(19):17060–17065.
26. Ji A, Dao D, Chen J, MacLellan WR (2003) EID-2, a novel member of the EID family of p300-binding proteins inhibits transactivation by MyoD. *Gene* 318:35–43.
27. Lee HJ, Lee JK, Miyake S, Kim SJ (2004) A novel E1A-like inhibitor of differentiation (EID) family member, EID-2, suppresses transforming growth factor (TGF)-beta signaling by blocking TGF-beta-induced formation of Smad3-Smad4 complexes. *J Biol Chem* 279(4):2666–2672.
28. Sasajima Y, Tanaka H, Miyake S, Yuasa Y (2005) A novel EID family member, EID-3, inhibits differentiation and forms a homodimer or heterodimer with EID-2. *Biochem Biophys Res Commun* 333(3):969–975.
29. Båvner A, Matthews J, Sanyal S, Gustafsson JA, Treuter E (2005) EID3 is a novel EID family member and an inhibitor of CBP-dependent co-activation. *Nucleic Acids Res* 33(11):3561–3569.
30. Guerineau M, et al. (2012) Analysis of the Nse3/MAGE-binding domain of the Nse4/EID family proteins. *PLoS One* 7(4):e35813.
31. Kozakova L, et al. (2015) The melanoma-associated antigen 1 (MAGEA1) protein stimulates the E3 ubiquitin-ligase activity of TRIM31 within a TRIM31-MAGEA1-NSE4 complex. *Cell Cycle* 14(6):920–930.
32. Hudson JJ, et al. (2011) Interactions between the Nse3 and Nse4 components of the SMC5-6 complex identify evolutionarily conserved interactions between MAGE and EID families. *PLoS One* 6(2):e17270.
33. Adelmant G, et al. (2012) DNA ends alter the molecular composition and localization of Ku multicomponent complexes. *Mol Cell Proteomics* 11(8):411–421.
34. Ficarro SB, et al. (2009) Improved electrospray ionization efficiency compensates for diminished chromatographic resolution and enables proteomics analysis of tyrosine signaling in embryonic stem cells. *Anal Chem* 81(9):3440–3447.
35. Askenazi M, Parikh JR, Marto JA (2009) mzAPI: A new strategy for efficiently sharing mass spectrometry data. *Nat Methods* 6(4):240–241.
36. Parikh JR, et al. (2009) multiplierz: An extensible API based desktop environment for proteomics data analysis. *BMC Bioinformatics* 10:364.
37. Rozenblatt-Rosen O, et al. (2012) Interpreting cancer genomes using systematic host network perturbations by tumour virus proteins. *Nature* 487(7408):491–495.
38. Kaelin WG, Jr, Pallas DC, DeCaprio JA, Kaye FJ, Livingston DM (1991) Identification of cellular proteins that can interact specifically with the T/E1A-binding region of the retinoblastoma gene product. *Cell* 64(3):521–532.
39. Geisen C, Moroy T (2002) The oncogenic activity of cyclin E is not confined to Cdk2 activation alone but relies on several other, distinct functions of the protein. *J Biol Chem* 277(42):39909–39918.